Combined Frequency and RoCoF Control of Converter-Interfaced Energy Storage Systems ⋆

Álvaro Ortega * **Federico Milano** *

* *School of Electrical & Electronic Engineering*
University College Dublin, Ireland
(e-mails: alvaro.ortegamanjavacas@ucd.ie; federico.milano@ucd.ie.)

Abstract: This paper proposes an effective control strategy for converter-interfaced energy storage systems to regulate simultaneously the frequency and its rate of change at the point of common coupling with the grid. The controller takes advantage of the fast response of CI-ESSs, and of the fact that the time frames of inertial response and primary frequency control are decoupled, allowing for an effective control capability the CI-ESS for both time frames after a disturbance. The performance of the proposed control is compared with the standard droop control and the popular virtual inertia provision. Simulation results, based on a modified version of the well-known WSCC 9-bus, 3-machine test system, indicate that the proposed control outperforms, for the scenarios considered, the other two control strategies.

Keywords: Frequency control, rate of change of frequency (RoCoF), converter-interfaced energy storage system (CI-ESS), battery energy storage, distributed energy resource (DER).

1. INTRODUCTION

The substitution of conventional synchronous generation with converter-interfaced generation (CIG) leads to the reduction of the total inertia of the system, which is one of the most limiting constraints to the integration of renewable resources based on wind and solar energy [Milano et al. (2018)].

There is an ongoing debate on the role of the controllers of the CIG as well as of converter-interfaced energy storage systems (CI-ESSs). In recent years, TSOs have recognized the need for new ancillary services, such as the Fast Responding Regulation Service (FRRS) defined by ERCOT already in 2002 [ERCOT Concept Paper (2013)], or the the Fast Frequency Response (FFR) defined by AEMO [Miller et al. (2017)]. A common feature of these definitions is the attempt to make a neat distinction between synchronous inertia response and frequency droop control.

This distinction often leads to impose that a certain fixed amount of energy has to be assigned to each service, regardless whether a device can provide more than one service at a time. This might not be the best approach as the inertial response or, in case of non-synchronous devices, RoCoF control, and frequency control are naturally decoupled due to their different transient behavior.

⋆ This material is based upon works funded by European Union's Horizon 2020 research and innovation programme under grant agreement No. 727481. F. Milano is also funded by the Science Foundation Ireland, grant No. SFI/15/IA/3074.
The opinions, findings, conclusions and recommendations expressed in this work are those of the authors and do not necessarily reflect the views of the European Union or Science Foundation Ireland. The European Commission and Science Foundation Ireland are not responsible for any use that may be made of the information that this work contains.

Another issue of some network codes is the assumption that the inertial response can be provided only by synchronous machines and the separation of this service from FFR [EirGrid and Soni (2012)]. Such a neat compartimentalization of services might not be the optimal strategy for highly controllable and flexible devices, such as CIG.

CIG, if operated with an adequate power reserve, can respond to RoCoF and frequency variations [Ochoa and Martínez (2017); Cerqueira et al. (2017)]. Virtual power plants are an example of combing together devices with different control purposes [Ruthe et al. (2012); Moutis and Hatziargyriou (2015); Etherden et al. (2016)]. However, it is also recognized that, due to their intermittent nature, most CIGs have a limited frequency control capability.

This is the crucial mission of CI-ESSs: to provide low-inertia power systems with the ability of maintaining the power balance during a transient in the interval of time between the end of the response of the transmission line dynamics (few milliseconds) and before the beginning of the response of primary frequency control (few seconds). Depending on the response times and capacities of the storage technology, CI-ESSs can provide either RoCoF control or frequency control, or both at the same time.

Fast frequency control of CI-ESSs is conceptually similar to the primary frequency control of synchronous machines (i.e., droop control). However, while the turbine governors of the synchronous machines require several seconds to start regulating, CI-ESSs can respond to frequency deviations much faster. Depending on the technology, the response time of CI-ESS droop control can span from a few tens of milliseconds (e.g., flywheels) to several hundred milliseconds or few seconds (e.g., batteries). In this time frame, the frequency is not the best quantity to be regulated due to its relatively slow time response. In fact,

to properly cope with frequency deviations shortly after a contingency, relatively high gains of the control are usually required, which may compromise the performance of the CI-ESS.

In low-inertia systems, the RoCoF shows high variations right after a large disturbance, which makes this quantity a good candidate for the regulation. With this regard, several configurations of RoCoF control for CI-ESSs have been proposed in the literature. The most common solution implies the use of hybrid CI-ESSs composed of two or more storage technologies with different response times (e.g., flywheel and battery). Then, the droop control is applied to the slowest storage device (battery, compressed air tank), and RoCoF control (more commonly known as virtual inertia control and synthetic inertia control) or alternatively fast frequency control to the fastest device (flywheel, electrochemical capacitor) [Fang et al. (2018); Abeywardana et al. (2017); Anzalchi et al. (2016)]. This solution, while generally effective, implies considerably high related costs. Moreover, electrochemical energy storage technologies have been undergoing significant research and development processes in recent years, which has allowed reducing the response times of batteries to less than a second, and the number of cycles during their operational life has substantially increased [IEC (2011)]. Other technologies, commonly seen as *fast but small* such as flywheels, are also undergoing a substantial improvement of their power and energy capacities. Therefore, the solution based on the coupling of fast and slow energy storage technologies will likely be outdated in the near future.

Another solution is to have only one CI-ESS behaving as a virtual synchronous generator, i.e., with virtual inertia response, leaving the responsibility of providing primary reserve to the synchronous machines of the system [Shi et al. (2018); Gonzalez-Longatt and Alhejaj (2016); Rubino et al. (2015)]. In this case, while the CI-ESS will show a good performance against fast frequency variations due to large contingencies, and lower related costs compared to hybrid solutions, it might not respond well to small or slow disturbances. This control is also highly sensitive to communication latency and jitter, as opposed to the intrinsic inertial response of synchronous machines which is instantaneous and always responding properly to power unbalances. Moreover, during a transient, the energy storage control can overlap with the droop control of the machines and, in some cases, these controls can send opposite orders to their respective devices. For example, during an under-frequency event, the droop control of the machines will try to move the frequency back to its reference value. This will cause a positive RoCoF, and thus, the CI-ESS will try to respond against it.

To prevent the last issue discussed above, an alternative control strategy considering a single CI-ESS has been proposed in [Toma et al. (2018)]. This strategy considers two input channels of the CI-ESS controller, one for the frequency deviation and another one for the RoCoF. This solution, as presented, poses several issues. First, no control is actually implemented other than the gains that define the participation of the CI-ESS to variations of each of the two input signals. Thus, no hard-limits and other non-linear dynamics typical of controllers for this type of applications (e.g., deadbands) are considered. The only dynamic of the CI-ESS modelled in [Toma et al. (2018)] is the time constant used to represent the overall behaviour of the storage device, and no reactive power support nor power converter dynamics are included. [Ortega and Milano (2016)] and references therein demonstrate that these overly-simplified CI-ESS models are not well suited for transient stability analysis.

The control strategy discussed in [Toma et al. (2018)] also intentionally constrains the regulation capability of the CI-ESS. For instance, the control is designed such that 20% of the regulation capability of the CI-ESS is used to help bringing the frequency value back to its reference few seconds after a large disturbance, while the remaining 80% is either inactive, or participating marginally after the time window of RoCoF control, i.e., up to few seconds after a disturbance. While obsequious of the network codes discussed above, this approach is unable to properly exploit the installed capacity of the storage device.

This paper proposes an efficient and effective control strategy, which takes advantage of the fact that the time frames of the RoCoF and droop controls are effectively decoupled. The proposed control has as unique input signal the frequency error. The error is then filtered and split in two channels, one for the *conventional* droop control, and the other one for the RoCoF, which includes a washout filter that computes the derivative of the frequency deviation. The main advantage of the control proposed is that it allows allocating, at any time, 100% of the regulation capability of the CI-ESS, thus optimizing its performance.

The paper is organized as follows. Section 2 highlights the model of a CI-ESS connected to the transmission grid. The proposed control strategy of CI-ESSs to regulate both the frequency and the RoCoF at the point of common coupling (PCC) is presented in Section 3. The case study based on the WSCC 9-bus, 3-machine benchmark network is provided in Section 4. Finally, Section 5 draws conclusions and future work directions.

2. MODELLING OF CONVERTER-INTERFACED ENERGY STORAGE SYSTEMS

The scheme of a CI-ESS connected to the transmission grid is shown in Fig. 1. The CI-ESS is composed of: (i) a storage device, e.g., a flywheel or a battery, (ii) a Voltage-Sourced Converter (VSC) that interfaces the storage device with the AC grid, (iii) the controllers of the VSC that regulate the DC- and AC-side voltages of the converter, and (iv) the active power control of the storage device.

There exists a large variety of CI-ESSs: batteries (lithium-ion, nickel-cadmium, etc.), flywheels, compressed air tanks, electrochemical capacitors, superconducting magnetic coils, and a large etc. Detailed transient stability models as well as more general, highly-simplified models have been proposed in the literature for all technologies above. For the purpose of the comparison presented in this paper, overly-simplified models are discarded, as accurate responses of the different storage technologies are required. Detailed transient stability models, on the other hand, are often cumbersome and require accurate parameter values. To overcome the issues above, in this paper, the generalized CI-ESS model (GEM) proposed in [Ortega and Milano

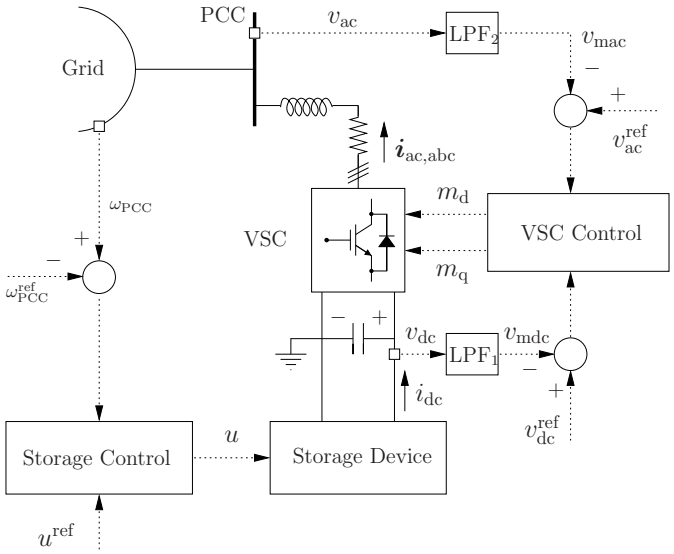

Fig. 1. Scheme of a CI-ESS connected to the transmission grid.

(2016)] is used. The models of the VSC and its controllers in the dq-reference frame are provided in [Yazdani and Iravani (2010); Chaudhuri et al. (2014)]. The overall model of the storage control scheme shown in Fig. 1 is described next.

3. RoCoF AND FAST PRIMARY FREQUENCY CONTROL OF CONVERTER-INTERFACED ENERGY STORAGE SYSTEMS

A simple two-channel controller for CI-ESSs aimed at regulating both the frequency and its rate of change has been recently proposed in [Toma et al. (2018)], and its scheme is shown in Fig 2. This strategy shows several limitations: (i) no control dynamics are considered; (ii) the model of the storage device is over-simplified; (iii) no reactive power support or interfacing converter is modelled; and (iv) the control capability of the CI-ESS is intentionally limited below its full potential for both channels.

The combined frequency and RoCoF control of CI-ESSs proposed in this paper is aimed at addressing the issues listed above. To regulate the charge and discharge processes (active power output) of the storage device, the PID control is the best known and most commonly used [Li et al. (2006); Molina et al. (2011)]. The proposed configuration of a PID-based frequency and RoCoF control of CI-ESSs is depicted in Fig. 3.

The controller takes, as single input, the error between the measured frequency at the PCC, ω_{PCC}, and its reference set-point, $\omega_{\text{PCC}}^{\text{ref}}$, and gives as output the variable of the storage device that regulates its active power output, u (e.g., the rotor angular speed of a flywheel).

The frequency error is passed through a deadband block and a low-pass filter (LPF) in order to reduce the sensitivity of the storage control to small, high-frequency perturbations such as noises. The aim of these blocks is to reduce the number of charge/discharge operations, thus increasing the life of the energy storage device.

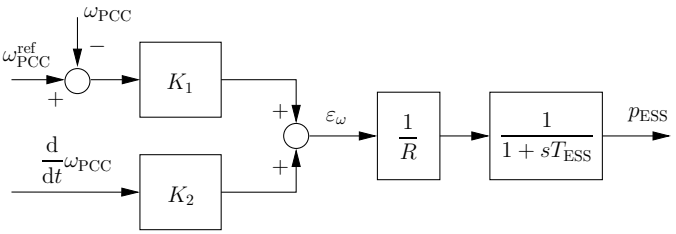

Fig. 2. Scheme of a simplified droop and RoCoF controller for CI-ESSs.

The output of the LPF, $x_{\text{f},u}$, is then used as input of two channels, one for the droop control with gain α, and another one for the RoCoF control, which computes the derivative of the filtered frequency error $x_{\text{f},u}$ by means of a washout filter. The RoCoF channel is disabled by imposing $K_{\text{r}} = 0$. The droop channel can be disabled if $\alpha = 0$.

The PID controller shown in Figure 3 is composed of a proportional gain, $K_{\text{p},u}$, an integrator with gain $K_{\text{i},u}$ and integral deviation coefficient $D_{\text{i},u}$, and a derivative gain $K_{\text{d},u}$. The coefficient $D_{\text{i},u}$ defines the steady-state error that is present in the droop control of synchronous machines. These parameters are commonly tuned by trial-and-error or pole-placement techniques. The simplicity of the implementation and design, as well as the ubiquitous utilisation of the PID control in industrial applications are its main strengths. Moreover, the structure of the PID control does not depend on the energy storage technology considered. Note that, if only the RoCoF channel is enabled, the integral deviation coefficient $D_{\text{i},u}$ must be set to 0 to avoid non-zero steady-state errors in the output of the controller, thus leading to a steady non-zero slope of the frequency. An alternative solution can be the use of a non-zero deadband (db).

The scheme shown in Fig. 3 also includes a block called Storage Input Limiter (SIL) [Ortega and Milano (2015)]. The purpose of the SIL is to reduce the impact of energy limits of the storage device on system transients.

4. CASE STUDY

Figure 4 shows the modified version of the well-known WSCC 9-bus [Sauer and Pai (1998)] used in this case study.

The modifications that have been conducted in this section with respect to the base case are listed below.

- The power base of the system has been reduced by 3 times, i.e., $S_n = 33.3$ MVA.
- The voltage of all transmission lines has been reduced by $\sqrt{3}$ times.
- The synchronous machine at bus 3 has been replaced by a wind power plant of the same capacity. The wind power plant is modelled as an aggregation of 18 fifth-order doubly-fed induction generators with optimal cubic MPPT approximation, first-order primary voltage regulation and static turbine governor.
- Due to the short simulation times considered, the wind is assumed to be constant.
- The loads are modelled as constant impedances.
- The voltage at the synchronous machine buses is reduced by 2% with respect to the base case.

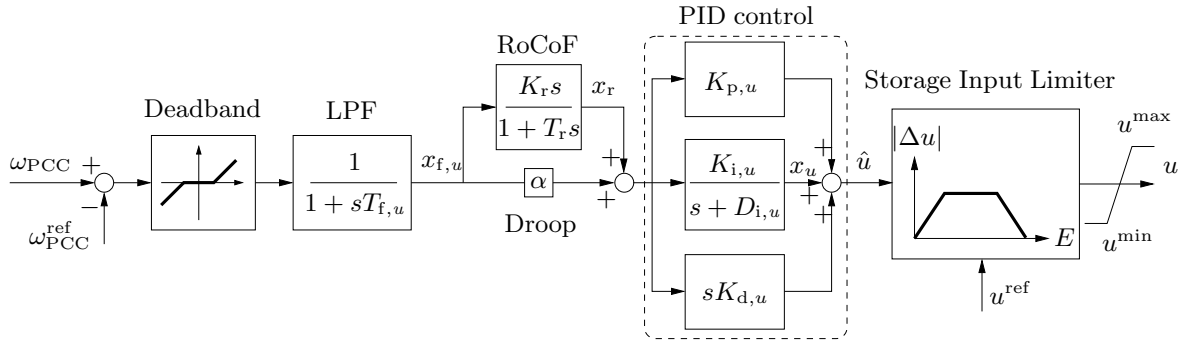

Fig. 3. Scheme of an enhanced droop and RoCoF controller for CI-ESSs.

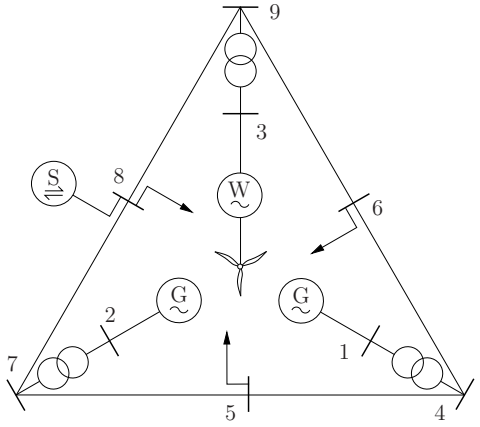

Fig. 4. Modified WSCC 9-bus, 3-machine system.

- The system includes a secondary frequency controller (AGC) with gain $K_o = 2$.
- The CI-ESS is connected to bus 8 through a 133/21 kV transformer.
- The frequency at the PCC is estimated by means of a phase-locked loop (PLL) device [Cole (2010)].
- The parameters of the PID control in Fig. 3 have been tuned by trial-and-error in order to obtain the best possible performance for each scenario.
- $D_{\mathrm{i},u} = 0.2$ and $db = 0$ have been used for the two cases with droop control, and $D_{\mathrm{i},u} = 0$ and $db = 0.0015$ if only the RoCoF channel is enabled.

Two main scenarios are considered. Subsection 4.1 considers a superconducting magnetic energy storage (SMES) system, while a battery energy storage (BES) system is simulated in Subsection 4.2. The aim of these two scenarios is to compare the performance of three CI-ESS control strategies, namely only droop, only RoCoF, and the combination of droop and RoCoF regulation, for energy storage technologies with different response times.

All simulations included in the paper are obtained using the Python-based software tool Dome [Milano (2013)]. The Dome version utilized is based on Ubuntu Linux 18.04, Python 3.6.7, CVXOPT 1.2.2, KLU 1.3.8, and MAGMA 2.2.0.

4.1 SMES

Figure 5(a) shows the transient response of the frequency at bus 8 of the WSCC system with and without an SMES system and various control strategies. The contingency

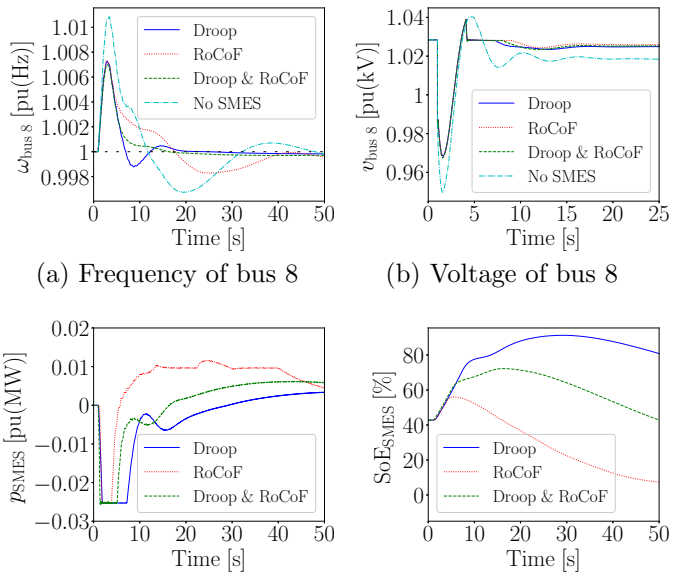

(a) Frequency of bus 8

(b) Voltage of bus 8

(c) SMES active power output

(d) SMES state of energy

Fig. 5. Response of the WSCC system with an SMES following a line outage for various frequency control strategies.

is the outage of the line connecting buses 4 and 5. The active power rate of the SMES is 2.5 MW. The best dynamic behaviour is obtained with the combined droop and RoCoF controller. While this had to be expected, it is interesting to note that the behaviour of the frequency in the first instants after the contingency is effectively the same for the three controllers. This is due to the fact that the SMES active power output saturates very quickly after the contingency (see Fig. 5(c)). A few seconds after the contingency, both strategies that include the droop channel show better performance than the one that only provides RoCoF control. This is also an expected result, as the RoCoF control does not prevent the synchronous machines to keep oscillating after the disturbance.

To better illustrate the differences between the three strategies during the first instants after the line outage, the power and energy capacities of the SMES are increased by 3 times, and results are shown in Figure 6. Again, the combination of RoCoF and droop control provides the best performance in both short-term and steady-state conditions. Installing an SMES with a larger power

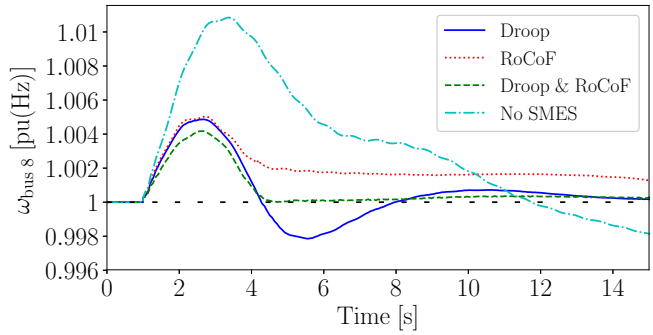

(a) Frequency at bus 8

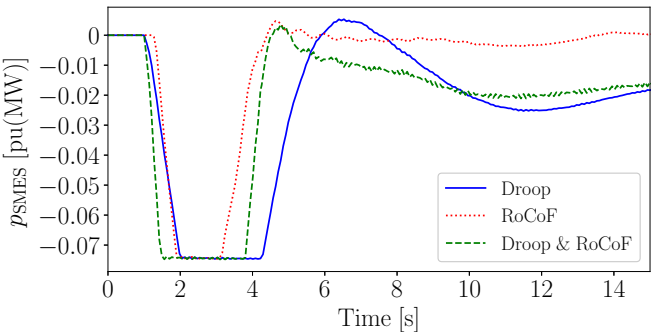

(b) SMES active power

Fig. 6. Response of the WSCC system with a large SMES following a line outage for various frequency control strategies.

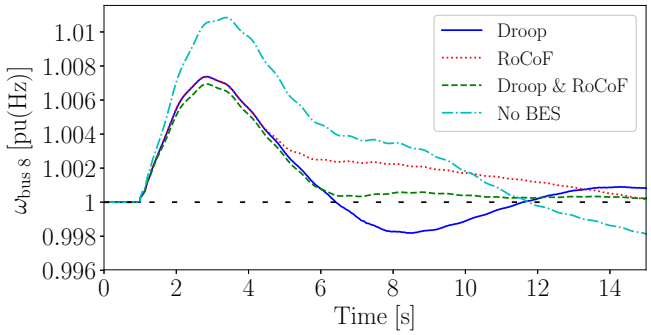

(a) Frequency at bus 8

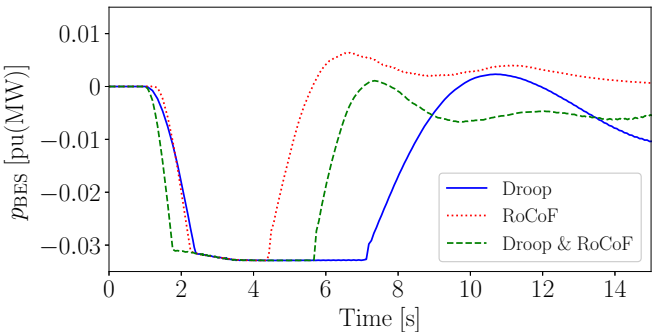

(b) BES active power

Fig. 7. Response of the WSCC system with a BES following a line outage for various frequency control strategies.

capacity allows for a substantial reduction of the slope of the frequency raise right after the line outage, thus reducing the RoCoF during these first instants. Moreover, this strategy shows the lowest frequency zenith and is the fastest to reach steady-state conditions. The other two strategies show a similar behaviour during the first two seconds. Figure 6(b) shows that, while the slope of the SMES active power right after the contingency is higher for the case where only the RoCoF channel is enabled compared to the case that includes only the droop control, the deadband introduces a latency that delays the control action. Finally, if only RoCoF control is enabled, the frequency steady-state value differs from the reference. Using only the RoCoF control of the SMES implies the need of waiting for the AGC to bring back the frequency to its reference value.

4.2 BES

In this scenario, a 3.2 MW BES is connected to bus 8. The contingency is again the outage of the line 4-5, and the response of the WSCC system without and with BES for the three control strategies compared in the previous subsection is shown in Fig. 7. Similar results to those obtained with the SMES are observed, being the combination of droop and RoCoF control the best strategy to regulate the frequency at the PCC, while the worst solution is to use only the RoCoF control. Note also that, despite having a response time substantially slower than the SMES (about an order of magnitude), the BES is able to provide a fairly good fast frequency control.

5. CONCLUSIONS

This paper proposes a fast frequency control strategy for CI-ESSs. This approach combines a droop and a rate of change of frequency regulation channels to optimize the performance of the controller. The proposed solution allows for a full control capability of the storage device for the time frames of both inertial response and primary frequency control. Simulation results show that the simplicity of the design and implementation of the control strategy do not compromise its performance thus providing a better tradeoff than other similar solutions previously proposed in the literature. Results also show that the proposed controller is effective for any kind of storage technology, regardless of their specific features such as response time, and power and energy capacities.

Future work will apply the proposed multi-channel controller to other frequency control strategies available for energy storage systems such as H-infinity, sliding mode and fuzzy logic controllers, which are claimed to be more robust than PID-based solutions.

Appendix A. ENERGY STORAGE SYSTEM DATA

Tables A.1 and A.2 show the data of the SMES and the BES devices, respectively, used in the simulations [Ortega and Milano (2016)]. The generalized CI-ESS model discussed in Section 2 also utilizes these data.

Table A.1. Data of the coil of the SMES device.

$i_{\mathrm{c}}^{\max}$ [kA]	$i_{\mathrm{c}}^{\min}$ [kA]	$i_{\mathrm{c,o}}$ [kA]	L_{c} [H]	R_{c} [Ω]
2.6	0.43	1.7	18.0	0

Table A.2. Data of a battery cell of the lithium-ion BES device ($n_{\mathrm{p}} = 60$, $n_{\mathrm{s}} = 640$).

$v_{\mathrm{b},n}$ [V]	Q_{n} [Ah]	$i_{\mathrm{b},n}$ [A]	$i_{\mathrm{b}}^{\max}$ [A]	R_{i} [Ω]	v_{e} [V]
2.3	30	30.0	120.0	$3.05{\cdot}10^{-4}$	0.1842
β_{e} [Ah^{-1}]	K_{p} [Ω]	R_{p} [Ω]	T_{m} [s]	$\mathrm{SoC}^{\min}$ –	$\mathrm{SoC}^{\max}$ –
2.0354	$4.06{\cdot}10^{-4}$	$4.06{\cdot}10^{-4}$	20.0	0.2	0.95

REFERENCES

Abeywardana, D.B.W., Hredzak, B., Agelidis, V.G., and Demetriades, G.D. (2017). Supercapacitor sizing method for energy-controlled filter-based hybrid energy storage systems. *IEEE Transactions on Power Electronics*, 32(2), 1626–1637.

Anzalchi, A., Pour, M.M., and Sarwat, A. (2016). A combinatorial approach for addressing intermittency and providing inertial response in a grid-connected photovoltaic system. In *2016 IEEE Power and Energy Society General Meeting (PESGM)*, 1–5.

Cerqueira, J., Bruzzone, F., Castro, C., Massucco, S., and Milano, F. (2017). Comparison of the dynamic response of wind turbine primary frequency controllers. In *Proceedings of the IEEE PES General Meeting*, 1–5.

Chaudhuri, N.R., Chaudhuri, B., Majumder, R., and Yazdani, A. (2014). *Multi-terminal Direct-current Grids: Modeling, Analysis, and Control*. John Wiley & Sons.

Cole, S. (2010). *Steady-State and Dynamic Modelling of VSC HVDC Systems for Power System Simulation*. Ph.D. thesis, Katholieke Universiteit Leuven.

EirGrid and Soni (2012). DS3: System Services Review TSO Recommendations. Technical report, EirGrid.

ERCOT Concept Paper (2013). Future Ancillary Services in ERCOT. Technical report.

Etherden, N., Vyatkin, V., and Bollen, M.H.J. (2016). Virtual power plant for grid services using IEC 61850. *IEEE Transactions on Industrial Informatics*, 12(1), 437–447.

Fang, J., Li, X., Tang, Y., and Li, H. (2018). Power management of virtual synchronous generators through using hybrid energy storage systems. In *2018 IEEE Applied Power Electronics Conference and Exposition (APEC)*, 1407–1411.

Gonzalez-Longatt, F.M. and Alhejaj, S.M. (2016). Enabling inertial response in utility-scale battery energy storage system. In *2016 IEEE Innovative Smart Grid Technologies - Asia (ISGT-Asia)*, 605–610.

IEC (2011). Electrical energy storage. Technical report, International Electrotechnical Committee. White Paper, available at: http://www.iec.ch.

Li, G., Cheng, S., Wen, J., Pan, Y., and Ma, J. (2006). Power system stability enhancement by a double-fed induction machine with a flywheel energy storage system. In *Proceedings of the IEEE PES General Meeting*.

Milano, F. (2013). A Python-based software tool for power system analysis. In *Proceedings of the IEEE PES General Meeting*.

Milano, F., Dörfler, F., Hug, G., Hill, D., and Verbič, G. (2018). Foundations and challenges of low-inertia systems. In *Proceedings of the Power Systems Computation Conference (PSCC)*, 1–22.

Miller, N., Lew, D., and Piwko, R. (2017). Technology capabilities for fast frequency response. Technical report, GE Energy Consulting.

Molina, M.G., Mercado, P.E., and Watanabe, E.H. (2011). Improved superconducting magnetic energy storage (SMES) controller for high-power utility applications. *IEEE Transactions on Energy Conversion*, 26(2), 444 – 456.

Moutis, P. and Hatziargyriou, N.D. (2015). Decision trees-aided active power reduction of a virtual power plant for power system over-frequency mitigation. *IEEE Transactions on Industrial Informatics*, 11(1), 251–261.

Ochoa, D. and Martínez, S. (2017). Fast-frequency response provided by DFIG-wind turbines and its impact on the grid. *IEEE Transactions on Power Systems*, 32(5), 4002–4011.

Ortega, Á. and Milano, F. (2015). Design of a control limiter to improve the dynamic response of energy storage systems. In *Proceedings of the IEEE PES General Meeting*.

Ortega, Á. and Milano, F. (2016). Generalized model of VSC-based energy storage systems for transient stability analysis. *IEEE Transactions on Power Systems*, 31(5), 3369–3380.

Rubino, S., Mazza, A., Chicco, G., and Pastorelli, M. (2015). Advanced control of inverter-interfaced generation behaving as a virtual synchronous generator. In *2015 IEEE Eindhoven PowerTech*, 1–6.

Ruthe, S., Rehtanz, C., and Lehnhoff, S. (2012). Towards frequency control with large scale virtual power plants. In *Proceedings of the IEEE PES Innovative Smart Grid Technologies Europe (ISGT Europe)*, 1–6.

Sauer, P.W. and Pai, M.A. (1998). *Power System Dynamics and Stability*. Prentice Hall, Upper Saddle River, NJ.

Shi, K., Ye, H., Song, W., and Zhou, G. (2018). Virtual inertia control strategy in microgrid based on virtual synchronous generator technology. *IEEE Access*, 6, 27949–27957.

Toma, L., Sanduleac, M., Baltac, S.A., Arrigo, F., Mazza, A., Bompard, E., Musa, A., and Monti, A. (2018). On the virtual inertia provision by BESS in low inertia power systems. In *2018 IEEE International Energy Conference (ENERGYCON)*, 1–6.

Yazdani, A. and Iravani, R. (2010). *Voltage-Sourced Converters in Power Systems – Modeling, Control and Applications*. Wiley-IEEE Press.